Underwater noise from glacier calving: Field observations and pool experiment

Oskar Glowacki

Citation: The Journal of the Acoustical Society of America **148**, EL1 (2020); doi: 10.1121/10.0001494
View online: https://doi.org/10.1121/10.0001494
View Table of Contents: https://asa.scitation.org/toc/jas/148/1
Published by the Acoustical Society of America

JASA EXPRESS LETTERS

https://doi.org/10.1121/10.0001494

Underwater noise from glacier calving: Field observations and pool experiment

Oskar Glowacki[a)]

Scripps Institution of Oceanography, University of California San Diego, La Jolla, California 92093-0206, USA
oglowacki@ucsd.edu

Abstract: The underwater noise emission from glacier calving is investigated by integrating acoustic and photographic observations made in a glacial bay and model pool. Similarities in the impact noise in these two settings are identified. Distinct fluid-dynamics processes are involved in sound generation: iceberg detachment, water entry, entrainment and collective oscillation of a bubble cloud, secondary impacts due to splashes, and calving-induced wave action. The lag between initial impact and bubble plume pinch-off from the subsurface cavity depends on ice block dimensions and drop height and may be useful in reducing errors in estimates of calving fluxes made using underwater sound.

[Editor: David R. Barclay] Pages: EL1–EL7

Received: 9 April 2020 **Accepted:** 10 June 2020 **Published Online:** 1 July 2020

1. Introduction

Glaciers worldwide are losing mass and contributing to sea-level rise.[1] Many of these glaciers terminate in the ocean, which makes them vulnerable to submarine melting and calving, the latter defined as the mechanical break-up of the ice edge. Recent studies have demonstrated that calving fluxes can be quantified through the analysis of underwater noise generated as icebergs impact onto the sea surface.[2,3] However, there is significant scatter in the noise energy between events of similar size and a better understanding of the mechanisms generating the impact noise is required to improve calving flux estimates. This issue is addressed here by combining acoustic and photographic observations made in a glacial bay and model pool. Similarities in the time- and frequency-structure of the impact noise generated at the fjord and pool scales are identified and linked to the evolution of the impact dynamics. The results can potentially be used to reduce the uncertainty in acoustic measurements of calving fluxes.

There are two major difficulties associated with quantifying glacier mass loss. First, unstable glacier termini prevent conducting *in situ* measurements at the ice cliff. Second, surface waves generated by calving icebergs pose a threat to boats. For these two reasons, and also because of the inaccessibility of most glaciers, remote sensing techniques are required to measure ice discharge. Moreover, glacier flow must be considered when estimating ice mass loss from changes of terminus position. Consequently, the application of satellite imagery for quantifying calving fluxes is limited by its spatial and temporal resolution. Other techniques, including time-lapse photography or laser scanning, are sensitive to weather and lighting conditions. These difficulties provide motivation to develop a new remote sensing tool for continuous and efficient monitoring of the ice loss.

Schulz *et al.*[4] were the first to propose acoustical oceanography as a potential tool for studying tidewater glacier dynamics. They encouraged the integration of acoustic monitoring with surface wave, temperature and salinity measurements in order to understand the mechanisms driving glacier retreat. Following this concept, independent studies conducted in Svalbard[5] and Alaska[6] reported the first measurements of the underwater noise from calving. Pettit[6] attributed the time- and frequency-varying signal to different source mechanisms, including ice fracturing, water entry, post-impact iceberg oscillation, and subsequent wave action. Glowacki *et al.* found a strong correlation between the kinetic energy of a falling iceberg and resulting low-frequency (<200 Hz) noise emission.[2] Encouraged by these findings, Glowacki and Deane analyzed 169 calving events and demonstrated that calving fluxes can be quantified from underwater noise made by icebergs impacting the sea surface.[3] The methodology was based on a robust power-law relationship between the impact energy and noise energy; the observed acoustic energy was corrected for propagation losses and contributions from

[a)]Also at: Institute of Geophysics, Polish Academy of Sciences, Warsaw, Poland, ORCID: 0000-0002-5164-0206.

terminus-reflected noise. The conversion efficiency from impact kinetic energy to acoustic energy was found to be 8×10^{-7}. Despite a strong correlation between the log-transformed variables ($r = 0.76$), impact noise energy varied roughly by a factor of 10 between icebergs of similar kinetic energy [see Fig. 7 in Glowacki and Deane[3]]. This inter-event variability in sound generation was attributed to different calving styles and associated source mechanisms. Consequently, low-error estimates of calving fluxes require a minimum number of calving observations; for example, 40 ice blocks result in a 20% uncertainty in iceberg mass flux at Hansbreen glacier, Svalbard. This requirement limits the temporal resolution of the acoustic technique, especially if calving activity at a particular location is low. However, it may be possible to lower the required sample size if the time-varying frequency structure of the impact noise contains information on a calving style.

The work presented here aims to address this issue by exploring distinct features of the calving signal and relating them to the impact dynamics. For this purpose, the existing theory for the sources of underwater noise from splashes (Sec. 2) is combined with noise measurements taken in two settings: a model pool and a glacial bay (Secs. 3 and 4).

2. Splashes as sources of underwater noise

Studies on splashes date back to 1908 when Worthington published remarkably sharp images of drops and solid spheres impacting liquid surfaces.[7] The complexity of the fluid-mechanical processes uncovered by these photographs inspired acousticians to investigate the impact noise.

A qualitative study on the subject by Mallock[8] was followed with observations of airborne noise from splashes made by several other authors. Most noticeably, Raman and Dey were the first to report that the sound generation depends largely on drop height and surface roughness of the impacting object.[9] In a following work by Richardson,[10] the underwater noise from impacts of solids onto the water surface was attributed to three major sources: an initial "slap" at the water entry, vibrations of the impacting object, and pulsations of an air cavity created by the impact. However, Franz made the striking observation that the third mechanism is associated with the oscillation of a bubble entrapped in water and not with the cavity.[11] At the time of this discovery, the resonant frequency of a single bubble pulsating underwater was already given by Minnaert.[12]

Although Franz wrongly hypothesized that the bubble entrainment is a random process, his finding was a milestone for our understanding of the sources of underwater noise from rainfall and breaking surface waves. The pulsation of the entrained bubble is—under some conditions—a predictable and regular mechanism responsible for the narrow 14-kHz peak in the rain noise spectrum, as demonstrated by Pumphrey and Crum.[13] The signal generated by the initial drop impact is still not well-understood, but it was found to be sharp, broadband, and contained strong near-field component.[14] Interestingly, Wenz proposed that the underwater sound from breaking waves is also largely generated by entrapped air.[15] The noise radiated above a few hundred hertz was later attributed to the pulsation of individual bubbles formed within a breaking wave crest.[16] Independent reports from Prosperetti[17] and Carey and Browning[18] suggested collective oscillations of bubble clouds as a mechanism that contributes to the low-frequency (<1 kHz) part of the wave noise spectrum. A pool experiment carried out by Kolaini and colleagues showed indeed narrow, low-frequency peaks in sound emission from bubble plumes created by impacting water jets.[19,20] They found that the emergence of this sound signature correlates well with bubble plume pinch-off from the subsurface cavity [see Fig. 1(c)]. The pinch-off process leads to the ejection of strong upward and downward jets.[7,21] The upward jet shoots from the water surface at the center of the splash crown and is widely known as the "Worthington jet" [see Figs. 2(a) and 1(d)]. Kolaini *et al.* proposed the downward jet as a mechanism that drives bubble plume into oscillation.[20] The resonant frequency of a spherical bubble cloud can be approximated by the modified Minnaert equation

$$f_0 \approx \frac{1}{2\pi R}\sqrt{\frac{3p_0}{\beta\rho}}, \tag{1}$$

where R is the radius of the plume, p_0 is the ambient pressure, ρ is the density of sea water, and β is the void fraction inside the bubble cloud.[22] Equation (1) gives a much lower frequency than would be expected from individual oscillations of bubbles creating the cloud.

Guided by these findings, sources of underwater noise from impacting icebergs are investigated here in order to improve the accuracy of acoustic measurements of calving fluxes. Experiments conducted in a model pool and glacial bay are described in Secs. 3 and 4.

JASA EXPRESS LETTERS
https://doi.org/10.1121/10.0001494

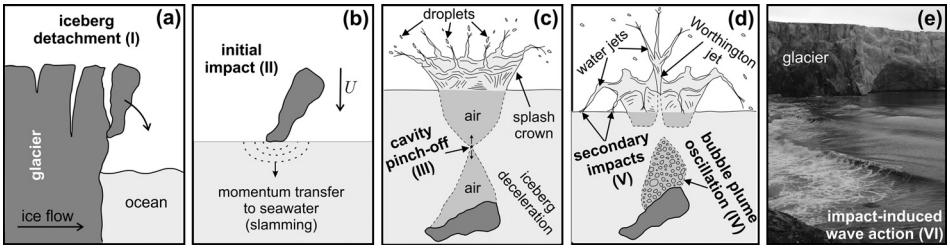

Fig. 1. (a)–(e) Sound-source mechanisms in subaerial calving ordered by the time of occurrence.

3. Pool experiment

Figure 2(a) shows a scheme of the experiment carried out in the OAR pool of the Scripps Institution of Oceanography, which was filled with seawater from around the SIO Pier. Five polypropylene- and two ice-cuboids and cylinders of different dimensions were dropped by hand onto the water surface in a total of 32 runs. Blocks of freshwater ice were purchased in a supermarket and then cut out into smaller cuboids. Vertical dimensions of the impacting blocks, L, varied from 0.04 to 0.32 m. The drop heights, h, measured as a vertical distance between the water surface and the midpoint of a block just before the drop, ranged from 1.02 to 2.95 m. Each impact event was photographed using two Redlake (now DEL Imaging Systems, Woodsville, NH, USA) MotionPro X3 high-speed cameras taking images at a maximum frame rate of 2000 Hz. Two example images of the splash crown and Worthington jet created by the impacting ice block are shown on the left-hand side of Fig. 2(a). Additionally, a GoPro (San Mateo, CA, USA) Hero 5 camera was mounted on an L-shaped frame and placed underwater to take pictures of the impact locations at a rate of 2 Hz. Noise measurements were also made from the frame with two International Transducer Corporation (Santa Barbara, CA, USA) 6050 C hydrophones spaced 0.6 m apart. High-speed camera data and sound recordings were synchronized using a Stanford Research Systems (Sunnyvale, CA, USA) DG645 pulse generator triggered by short impulses of the initial impacts. The reverberation effects of the pool were not evaluated because the present study focuses on the time-varying frequency structure of the signal and not on the absolute noise levels.

4. Field observations of calving events

Underwater noise measurements were made in the summer of 2016 in Hornsund fjord, Svalbard with a High Tech (Long Beach, MS, USA) 96-MIN hydrophone. The mooring equipped with the acoustic recorder was deployed at a depth of 40 m and around 1000 m from the terminus of Hansbreen glacier ["H" in Fig. 2(b)]. The glacier front was photographed with a GoPro Hero 3+ camera that took images at a rate of 1 Hz ["CAM" in Fig. 2(b); see example images in Figs. 3(b) and 3(c)]. Camera data were synchronized with noise recordings by matching images of

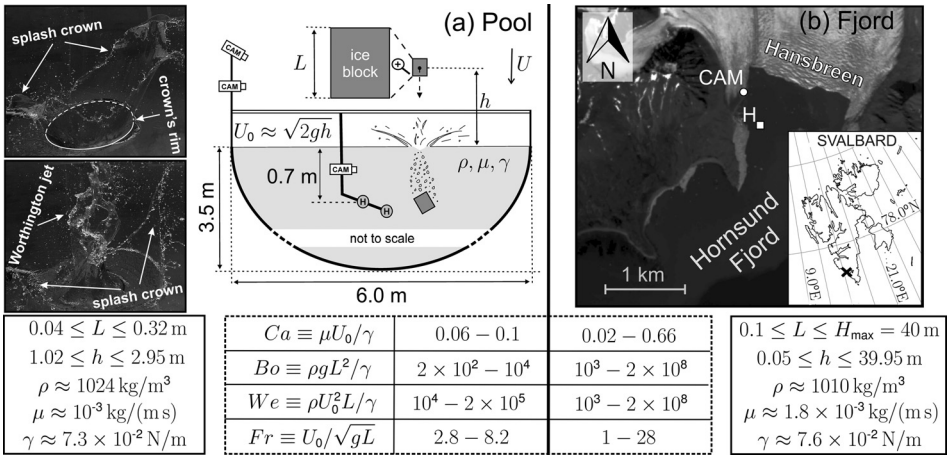

$0.04 \le L \le 0.32\,\mathrm{m}$ $1.02 \le h \le 2.95\,\mathrm{m}$ $\rho \approx 1024\,\mathrm{kg/m^3}$ $\mu \approx 10^{-3}\,\mathrm{kg/(m\,s)}$ $\gamma \approx 7.3 \times 10^{-2}\,\mathrm{N/m}$	$Ca \equiv \mu U_0/\gamma$	$0.06 - 0.1$
	$Bo \equiv \rho g L^2/\gamma$	$2 \times 10^2 - 10^4$
	$We \equiv \rho U_0^2 L/\gamma$	$10^4 - 2 \times 10^5$
	$Fr \equiv U_0/\sqrt{gL}$	$2.8 - 8.2$

$0.02 - 0.66$	$0.1 \le L \le H_{\max} = 40\,\mathrm{m}$ $0.05 \le h \le 39.95\,\mathrm{m}$ $\rho \approx 1010\,\mathrm{kg/m^3}$ $\mu \approx 1.8 \times 10^{-3}\,\mathrm{kg/(m\,s)}$ $\gamma \approx 7.6 \times 10^{-2}\,\mathrm{N/m}$
$10^3 - 2 \times 10^8$	
$10^3 - 2 \times 10^8$	
$1 - 28$	

Fig. 2. (a) A schematic of the pool experiment and (b) a map of the glacial bay. Locations of cameras and hydrophones are marked as CAM and H, respectively. Example images of the block-water impact are shown on the left-hand side of panel (a). Value ranges of non-dimensional parameters are given at the bottom. The maximum height of the glacier terminus is assumed to be $H_{\max} = 40$ m and the lower limit of the vertical dimension of the ice block in the bay is set to 0.1 m. The approximated value of the impact velocity is given by $U_0 \approx \sqrt{2gh}$, where $g = 9.81$ m/s^2 is the acceleration due to gravity. Estimated water properties are: ρ—density, μ—viscosity, and γ—surface tension.

small ice blocks falling onto the water surface with the resulting short pulses of sound radiated by the impacts. Details of the field experiment are described more thoroughly in Glowacki and Deane.[3]

A similarity between the impact dynamics at two different scales of the model pool and glacial bay can be interpreted using non-dimensional numbers: Capillary (*Ca*; viscous force/surface tension), Bond (*Bo*; gravitational force/surface tension), Weber (*We*; inertia force/surface tension), and Froude (*Fr*; inertia force/gravitational force) (see Fig. 2 for definitions). Parameter values at the pool scale are usually between the limits obtained for field observations (Fig. 2). A cavity pinching off one-third to one-half of a distance from the ice block up to the sea surface (deep seal scenario) is expected for Bond and Froud numbers considered here (typically $Bo > 10\,000$ and $Fr < 12$) (see Truscott *et al.*[21] and references therein). This type of cavity closure—driven by the hydrostatic pressure that pushes air/liquid interface radially inward—will now be assumed [see Fig. 1(c)]. However, two issues resulting from this simplification have to be borne in mind. First, conditions for the deep seal scenario are not always met for small ice blocks ($L < 1$ m) breaking high enough from the glacier terminus ($h > 7$ m). In such cases the cavity most likely closes at the free surface (surface seal scenario) (see, for example, Figs. 3 and 4 in Truscott *et al.*[21]), which may largely affect the noise emission (e.g., source depth and propagation conditions). Second, the impact velocity (and resulting *Ca* and *We*) can be too small for cavity creation, or positive buoyancy of the ice may—under some impact conditions—prevent the total submergence of the block and bubble plume entrainment.

Section 5 discusses distinct features of the impact noise and associated fluid-dynamics processes. Their relevance for improving acoustic estimates of calving fluxes is also considered.

5. Sound-source mechanisms in subaerial calving

Calving events radiate underwater noise that varies greatly with time and frequency.[2,3,5,6] The variability in the calving signal almost certainly results from the evolution of different mechanisms of noise generation. The complexity of this process is revealed by sound recordings synchronized with time-lapse images of icebergs falling onto the sea surface (see supplementary movies in Glowacki *et al.*[2]). Figure 1 shows major phases of subaerial calving in terms of noise emission, as deduced from observations made in the glacial bay and model pool.

First, the iceberg fractures, breaks-off from the glacier terminus, and starts to fall towards the ocean [mech. I, Fig. 1(a)]. Second, the falling iceberg strikes the sea surface and transfers momentum ("slamming force") to the water column [mech. II, Fig. 1(b)]. This stage is followed by the creation of the splash crown and subsurface cavity [Figs. 2(a) and 1(c)]. After the ice block is totally submerged, the cavity pinches off and a bubble cloud is entrained [mech. III, Figs. 1(c) and 1(d) and Fig. 3(a)]. Immediately after the cavity pinch-off, the bubble plume is

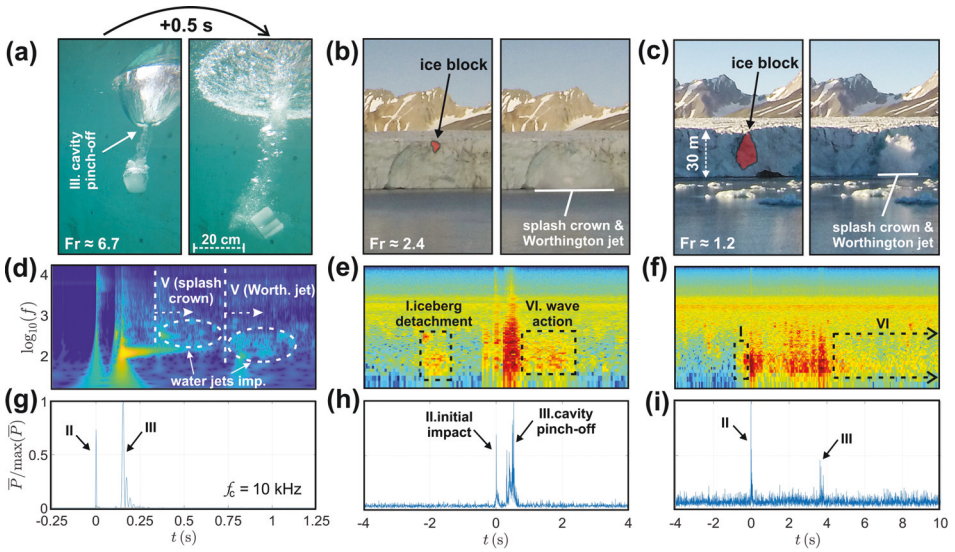

Fig. 3. Three distinct scenarios of the block-water impact: (left) an ice block dropped into the model pool, (middle) a small block of ice falling from the top of the glacier terminus, and (right) a big iceberg impacting the sea surface. (a) Underwater images of the cavity pinch-off and entrained bubble cloud. (b) and (c) Images of the glacier terminus. (d) A scalogram of the impact noise generated by the ice block falling into the pool. (e) and (f) Spectrograms of the underwater noise radiated by calving events. (g)–(i) Time series of the normalized, average noise power computed over one-third octave band centered at 10 kHz.

JASA EXPRESS LETTERS
https://doi.org/10.1121/10.0001494

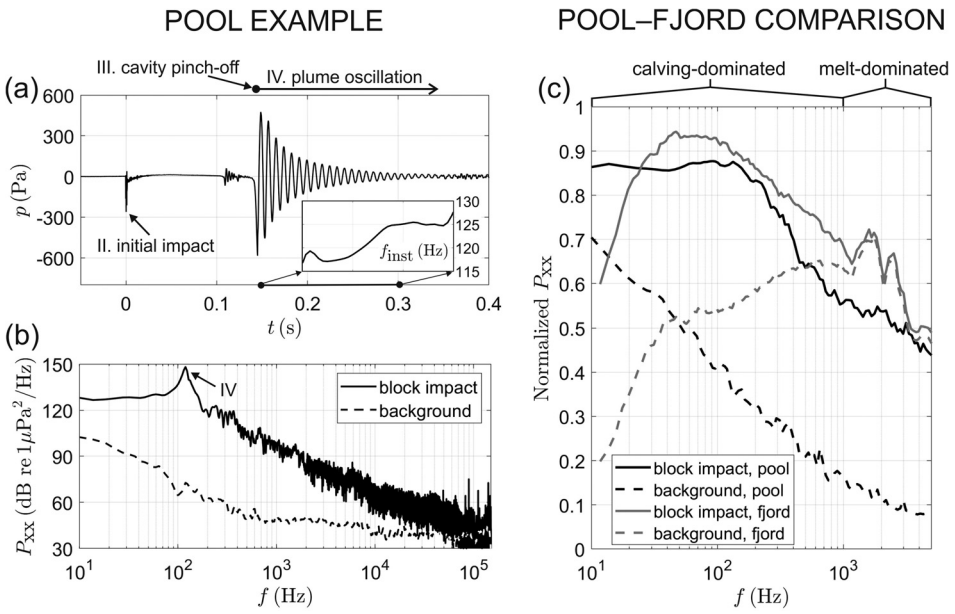

Fig. 4. (a) and (b) An example of the acoustic pressure time series and time-averaged power spectrum of the impact noise recorded in the pool. The inset of (a) shows a shift in the oscillation frequency. (c) A comparison between median, min–max normalized power spectral densities for 32 and 169 impacts observed, respectively, in the model pool (black) and in the glacial bay (gray).

driven into acoustic oscillation, most likely by a downward water jet,[20] and radiates sound at a frequency given by Eq. (1) [mech. IV, Fig. 1(d)]. Additionally, the Worthington jet is ejected upwards [Figs. 2(a), 1(d) and Figs. 3(b) and 3(c)]. Then, secondary impacts due to splashes are expected, with droplets and water jets from the splash crown preceding those from the Worthington jet [mech. V, Fig. 2(a) and 1(d)]. Finally, impact-induced surface waves interact with the shore, glacier terminus, and ice floating on the sea surface [mech. VI, Fig. 1(e)]. The lapping of wave crests on the underside of the periphery of icebergs is a potential source of underwater noise at frequencies between 100 and 500 Hz, as demonstrated by Deane *et al.*[23] Distinct features of the calving noise will now be considered.

Figure 4(a) shows an example of the impact noise generated by the ice block falling into the pool. Two major components of the unfiltered waveform are clearly noticeable: a sharp increase of the sound pressure at the water entry and a much longer, low-frequency signal from damped oscillation of the bubble plume (mech. II and IV, respectively). Due to the high clarity of the pool water, it was possible to observe the exact pinch-off time using high-speed cameras (mech. III). Similar patterns of the underwater noise generated by impacting solids, drops, and water jets have been observed by many authors, including early investigators.[10,11,19,20] The inset of Fig. 4(a) presents an instantaneous frequency of the oscillation component. A frequency shift from around 117 to 127 Hz is evident as the pressure decays in time. A similar increase in frequency was also observed by Kolaini for water jets, who attributed this effect to the expansion of the bubble plume containing a constant volume of air [see Eq. (1)].[20] This explanation for the frequency shift is consistent with underwater images of the bubbly region taken in this study [Fig. 3(a)]. A narrow, low-frequency peak of the plume oscillation is a dominant feature of the noise spectrum [Fig. 4(b)]. However, the sound radiated from the block impact covers a broad range of frequencies. Figure 4(c) compares median, min–max normalized noise spectra for 32 impacts recorded in the pool (black) and for 169 subaerial calving events observed in the glacial bay (gray). In both settings the impact noise has a pronounced peak centered at around 100 Hz, which is most likely due to the volume oscillations of the plumes. The peak in fjord observations is shifted to lower frequencies in comparison with the pool measurements. According to Eq. (1), this effect is presumably the result of the much larger plumes created by icebergs, with the assumption of similar void fractions. At frequencies above 1 kHz, the underwater noise in the bay is typically dominated by pressurized gas bubbles bursting from the glacier ice as it melts.[24] This component of the Arctic soundscape has well-pronounced peaks between 1 and 3 kHz [Fig. 4(c)], as shown by Deane *et al.*[23] and Pettit *et al.*[25]

The initial impact and damped oscillation of a bubble plume are two of the processes generating the calving noise but there are more (Fig. 1). The time and frequency structure of the calving noise will now be discussed in order to identify and explore the remaining signatures.

Figure 3 shows examples of three distinct impact scenarios in terms of the Froude number: (a) an ice block dropped into the model pool; $Fr \approx 6.7$, (b) a small block of ice falling from the top of the glacier terminus; $Fr \approx 2.4$ (b), and (c) a big iceberg breaking off and striking the sea surface; $Fr \approx 1.2$. There are two patterns in the calving signal that cannot be observed in the pool but are clearly identified in the spectrograms of the noise recorded in the bay: detachment of an ice block from the glacier terminus (mech. I) and interactions of the impact-driven surface waves with the shore, ice front and floating icebergs (mech. VI) [Figs. 1(a) and 1(e)]. The duration (and overall level) of the noise emission from wave action clearly increases with increasing impact kinetic energy but these signatures certainly depend also on the amount of ice on the sea surface and cannot be used as a proxy for block dimensions or drop height. Similarly, the low-frequency signal of the block detachment potentially results from the vibration of the glacier terminus and is unrelated to the block dynamics. Other processes that likely contribute to the calving noise are, for example, vibrations of the ice block, interactions between the iceberg and glacier terminus, and pulsations of individual bubbles at the plume boundary and its close proximity. Friction between the iceberg and glacier terminus may be responsible for exciting the low-frequency sounds radiated between the initial impact and cavity pinch-off [see 0.1–3.5 s of the spectrogram in Fig. 3(f)]. Splashes are also involved in noise emission as droplets and ribbon-like filaments of different scales originating from the crown and Worthington jet fall onto the water surface [mech. V; Figs. 2(a) and 1(d)]. Acoustic signatures of these secondary impacts are clearly visible in a less noisy environment of the model pool and can be separated in terms of their origin [impacts due to the splash crown emerge first; Fig. 3(d)]. Moreover, impacting water jets generate lower frequency sounds ($<$500 Hz) than small droplets, as predicted by Eq. (1) [see ellipses in Fig. 3(d)].

Interestingly, a combination of high-speed photography and synchronized acoustic recordings taken in the pool revealed broadband, short peaks in noise power at the initial impact and cavity pinch-off [Fig. 3(d); see 0 and 0.15 s of the scalogram, respectively]. The wide range of frequencies radiated by the initial impact was observed by early investigators of the rain noise, including Franz[11] and Pumphrey.[14] The latter author suggested that the pulse has a very strong near-field component, but the present study demonstrates a clear signal of the water entry picked up by a distant receiver in the glacial bay. Signatures of the initial impact and cavity pinch-off are found on spectrograms of the calving noise at frequencies above a few kHz, where the melt signal still exists but is not so dominant[23,25] [Figs. 3(e) and 3(f); see also Fig. 4(c)]. These patterns are even more pronounced in time series of normalized, average noise power over a one-third octave band centered at 10 kHz [Figs. 3(g)–3(i)]. The separation between the initial impact and cavity pinch-off increases with decreasing Froude number, which results from the extension of time required for the total submergence of the ice block. Significantly, the impact-to-pinch-off time delay couples high-frequency structure of the impact noise with the unique features of impact dynamics: drop height and iceberg dimensions. Therefore, automatic recognition of the initial impact and cavity pinch-off in the calving signal can be potentially used to improve acoustical measurements of calving fluxes. This improvement can be achieved by reducing the uncertainty associated with the large variability in impact noise energy generated by icebergs of similar kinetic energies but different calving styles (roughly an order of magnitude for Hansbreen glacier, Svalbard[3]). Importantly, impacts of small ice blocks breaking off just above the sea surface have low Froude numbers, but do not generate much noise above the background level and cannot be mistaken with large calving events. It is also worth mentioning that the existence of more than two high-frequency peaks in the calving signal may be an indicator of iceberg fragmentation and the resulting change of calving mode from a single impact to the form of an avalanche.

6. Concluding remarks

A combination of experiments conducted in a model pool and glacial bay has demonstrated distinct mechanisms of underwater noise emission from subaerial calving, including: iceberg detachment, initial impact, pinch-off and collective oscillation of a bubble plume, secondary impacts due to splashes, and calving-induced wave action. Importantly, time- and frequency-structure of the impact noise is similar at these two different scales. The lag between initial impact and cavity pinch-off is a function of iceberg dimensions and drop height, and can potentially be used to lower the uncertainty in acoustic estimates of calving fluxes. It is also possible that other features of the impact noise can be useful. For example, frequency of the bubble plume oscillation may be a proxy for the ice discharge, provided that the void fraction is relatively constant (or predictable) and the plume size scales with the iceberg volume [see Eq. (1)]. Moreover, some of the sound-source mechanisms in subaerial and submarine calving are likely different (e.g., lack of air cavity after broaching), potentially allowing these two sources of ice loss to be acoustically distinguished and quantified. Future work will test these possibilities.

https://doi.org/10.1121/10.0001494

Acknowledgments

The author is grateful to Dr. Grant Deane for a number of helpful discussions that inspired this work, and Philip Tuckman who assisted with the data collection during the pool experiment. It is a pleasure to acknowledge the work of Dr. Mateusz Moskalik who oversaw the oceanographic monitoring in Hornsund fjord, and the support of the staff at the Polish Polar Station Hornsund. The helpful comments and suggestions provided by Dr. Philippe Blondel and an anonymous reviewer are greatly appreciated. This work has been supported by the Ministry of Science and Higher Education of Poland (Grant No. 1621/MOB/V/2017/0 and statutory activities Grant No. 3841/E-41/S/2016), the U.S. Office of Naval Research (Grant No. N00014-17-1-2633), and the U.S. National Science Foundation (Grant No. OPP-1748265).

References and links

[1]M. Zemp, M. Huss, E. Thibert, N. Eckert, R. McNabb, J. Huber, M. Barandun, H. Machguth, S. U. Nussbaumer, I. Gärtner-Roer, L. Thomson, F. Paul, F. Maussion, S. Kutuzov, and J. G. Cogley, "Global glacier mass changes and their contributions to sea-level rise from 1961 to 2016," Nature **568**, 382–386 (2019).

[2]O. Glowacki, G. B. Deane, M. Moskalik, P. Blondel, J. Tegowski, and M. Blaszczyk, "Underwater acoustic signatures of glacier calving," Geophys. Res. Lett. **42**(3), 804–812, https://doi.org/10.1002/2014GL062859 (2015).

[3]O. Glowacki and G. B. Deane, "Quantifying iceberg calving fluxes with underwater noise," Cryosphere **14**(3), 1025–1042 (2020).

[4]M. Schulz, W. H. Berger, and E. Jansen, "Listening to glaciers," Nat. Geosci. **1**, 408 (2008).

[5]J. Tegowski, G. B. Deane, A. Lisimenka, and P. Blondel, "Spectral and statistical analyses of ambient noise in Spitsbergen Fjords and identification of glacier calving events," in *Proceedings of the Institute of Acoustics 11th European Conference on Underwater Acoustics 2012*, St. Albans (2012), pp. 1667–1672.

[6]E. C. Pettit, "Passive underwater acoustic evolution of a calving event," Ann. Glaciol. **53**(60), 113–122 (2012).

[7]A. M. Worthington, *A Study of Splashes* (Longmans, Green, and Company, London, United Kingdom, 1908), 129 pp.

[8]A. Mallock, "Sounds produced by drops falling on water," Proc. R. Soc. London Set. A **95**(667), 138–143 (1918).

[9]C. V. Raman and A. Dey, "On the sounds of splashes," Phil. Mag. **39**(229), 145–147 (1920).

[10]E. G. Richardson, "The impact of a solid on a liquid surface," Proc. Phys. Soc. **61**(4), 352–367 (1948).

[11]G. J. Franz, "Splashes as sources of sound in liquids," J. Acoust. Soc. Am. **31**(8), 1080–1096 (1959).

[12]M. Minnaert, "On musical air bubbles and the sounds of running water," Phil. Mag. **16**(104), 235–248 (1933).

[13]H. C. Pumphrey and L. A. Crum, "Acoustic emissions associated with drop impacts," in *Sea Surface Sound*, NATO ASI Series, edited by B. R. Kerman (Springer, Dordrecht, 1988), pp. 463–483.

[14]H. C. Pumphrey, "Sources of underwater rain noise," in *Natural Physical Sources of Underwater Sound*, edited by B. R. Kerman (Springer, Dordrecht, 1993), pp. 683–696.

[15]G. M. Wenz, "Acoustic ambient noise in the ocean: Spectra and sources," J. Acoust. Soc. Am. **34**(12), 1936–1956 (1962).

[16]H. Medwin and M. M. Beaky, "Bubble sources of the Knudsen sea noise spectra," J. Acoust. Soc. Am. **86**(3), 1124–1130 (1989).

[17]A. Prosperetti, "Bubble-related ambient noise in the ocean," J. Acoust. Soc. Am. **84**(3), 1042–1054 (1988).

[18]W. M. Carey and D. Browning, "Low-frequency ocean ambient noise: Measurement and theory," in *Sea Surface Sound*, NATO ASI Series (Springer, Dordrecht, 1988), pp. 361–376.

[19]A. R. Kolaini, R. A. Roy, and L. A. Crum, "An investigation of the acoustic emissions from a bubble plume," J. Acoust. Soc. Am. **89**(5), 2452–2455 (1991).

[20]A. R. Kolaini, R. A. Roy, L. A. Crum, and Y. Mao, "Low-frequency underwater sound generation by impacting transient cylindrical water jets," J. Acoust. Soc. Am. **94**(5), 2809–2820 (1993).

[21]T. T. Truscott, B. P. Epps, and J. Belden, "Water entry of projectiles," Ann. Rev. Fluid Mech. **46**, 355–378 (2014).

[22]W. M. Carey, J. W. Fitzgerald, E. C. Monahan, and Q. Wang, "Measurement of the sound produced by a tipping trough with fresh and salt water," J. Acoust. Soc. Am. **93**(6), 3178–3192 (1993).

[23]G. B. Deane, O. Glowacki, J. Tegowski, M. Moskalik, and P. Blondel, "Directionality of the ambient noise field in an Arctic, glacial bay," J. Acoust. Soc. Am. **136**(5), EL350–EL356 (2014).

[24]P. F. Scholander, J. W. Kanwisher, and D. C. Nutt, "Gases in icebergs," Science **123**, 104–105 (1956).

[25]E. C. Pettit, K. M. Lee, J. P. Brann, J. A. Nystuen, P. S. Wilson, and S. O'Neel, "Unusually loud ambient noise in tidewater glacier fjords: A signal of ice melt," Geophys. Res. Lett. **42**(7), 2309–2316, https://doi.org/10.1002/2014GL062950 (2015).